Morphological and anatomical characterization of *Actinidia kolomikta* (Rupr. & Maxim.) Maxim. (C3) and *Amaranthus tricolor* L. (C4) leaves

S. Motyleva[1,*], E. Vlasova[1], N. Kozak[1], M. Gins[2] and V. Gins[2]

[1]Federal Horticultural Research Center for Breeding, Agrotechnology and Nursery, 4 Zagorevskaj Str., RU115598 Moscow, Russia
[2]Federal Scientific Center of Vegetable Growing, 14 Selectnaya Str., Moscow region, Odintsovsky urban district, RU143080 VNIISSOK village, Russia
[*]Correspondence: motyleva_svetlana@mail.ru

Abstract. Morphological and anatomical features of new cultivars with photosynthesis of C3 (*Actinidia kolomikta* (Rupr. & Maxim.) Maxim. cv. 'Narodnaya') and C4 (*Amaranthus tricolor* L. cv. 'Valentina') were established by light and scanning electron microscopy, as well as energy-dispersive analysis. The leaf lamina of *Actinidia kolomikta* cv. 'Narodnaya' has a dorsoventral anatomical structure, anomocytic stomata on the abaxial epidermis and two types of trichomes: multicellular, uniseriate hairs and multicellular bristle-like protrusions, containing raphids. The needle-like raphides are located in subepidermal layers along the veins. A vascular system of petiole consists of two upper concentric bundles and the crescentic vascular strand. A starch sheat is present. Raphides (needle-shaped and rectangular) are located in phloem and cortical parenchyma cells, contain Ca, K, Mg, P and Si. The leaf lamina of *Amaranthus tricolor* cv. 'Valentina' have the kranz-anatomy, dorsiventral mesophyll and contain druses. Betacyanins are concentrated in the epidermis and mesophyll, but are not present in the bundle sheath. The number of vascular bundles in petioles is odd-numbered and variable (from 5 to 13). Trichomes are multicellular, uniseriate, ending in a large oval cell. Cells with betacyanins are present in the epidermis cortex, and, rarely, the collenchyma and phloem of the petiole. Cells with betaxanthins are absent. A starch sheat is brightly pigmented with betacyanins. The crystall sand is deposited in the parenchyma cells of the cortex and pith of the petiole and contains Ca (mainly) and K oxalates. Druses in the leaf lamina additionally contain Mg and P.

Key words: *Actinidia kolomikta* (Rupr. & Maxim.) Maxim., *Amaranthus tricolor* L., leaf, mineral inclusions, morphology, betacyanins, light microscopy, scanning electron microscopy, energy dispersive analysis.

INTRODUCTION

An anatomical and morphological survey in plant breeding is carried out for identify signs of authenticity of new varieties, markers of adaptability, as well as limits of intraspecific variability (Lotova, 2011; Crivellaro & Schweingruber, 2015; Durnova et al., 2021).

The accumulation of calcium oxalate crystals is a normal activity closely integrated with metabolism of the photosynthetic organisms. It has been suggested that crystals play a significant role in maintaining the ion balance of the cell, in plant protection, in mechanical support of tissues, in detoxification, in light harvesting and reflection (Franceschi & Horner, 1980; Semenova & Romanova, 2011). However, the causes of the crystal formation and their physiological role remain insufficiently established (McConn & Nakata, 2002).

Another controversial issue is the physiological role of betalains and anthocyanins in the vegetative organs of plants. These substances, which have antioxidant properties, are thought to increase the photostability of leaves and stems, to protect against increased levels of UV radiation, and to defense against pathogenic fungal infection (Close & Beadle, 2003; Solovchenko & Merzlyak, 2008; Flexas et al., 2012).

The life-forms of the *Actinidiaceae* Gilg & Werderm. are represented by perennial woody vines and shrubs with climbing shoots. These plants use C3 photosynthesis. The anatomical structure of the stem of *Actinidia kolomikta* (Rupr. & Maxim.) Maxim is typical for dicotyledonous plants. Collateral vascular tissues without separate bundles are arranged in a ring around the core (Condon, 1992; Clearwater & Clark, 2003; Roy et al., 2020). There are raphides and mucilage in shoots and leaves (Ferguson, 2011). White and pink areas appear on the green leaves during the budding - flowering phase. The bleaching areas of leaves turn pink if they are in direct sunlight. The pink color of the leaves is associated with anthocyanins synthesis (Kolbasina et al., 2007; Wang et al., 2015).

The genus *Amaranthus* L. differs from typical dicotyledonous plants by many physiological and anatomical characteristics. Amaranth is characterized by high drought, thermal and salt resistance thanks to C4 photosynthesis. Leaves are characterized by Kranz anatomy, where mesophyll cells are grouped around the cells of the bundle-membrane in a ring-like manner. This structure contributes to a faster outflow of photosynthetic products compared to C3 species (Chirkova, 1999; Zhigila et al., 2014). Amaranth leaf mesophyll contains calcium oxalate crystals (Tooulakou et al., 2016). Leaves of *Amaranthus tricolor* L. have many colors, often variegated. The purple-red color is associated with the presence of betacyanins in the vacuoles of cells, which are represented by amaranthin and isomaranthin. The presence of yellow shades is associated with the presence of betanin, iso-betanin (betaxanthins). The *Amaranthus tricolor* L. leaves also contain abundant amounts of photosynthetic and non-photosynthetic carotenoids and chlorophylls (Cai et al., 1998, 2005; Sarker & Oba, 2020a). *Amaranthus* L. species with red color of vegetative organs (*A. tricolor* L., *A. gangeticus* L.) as a rule surpasses green-leaved species (*A. dibius* K. Krause, *A. lividus* L., *A. hypochondriacus* L.) in terms of the antioxidant capacity, the total content of phenolic compounds, flavonoids, carotenoids and betalains. A high thermal and salt tolerance of *Amaranthus tricolor* L. is associated with these substances (Shu et al., 2009; Khanam & Oba, 2013; Hoang et al., 2019; Sarker & Oba, 2019a, 2019b; 2020d). In particular, an increase in the content of phenolic acids, ascorbic acid, rutin, isoquercetin, nonenzymatic antioxidants (ascorbate, carotenoids), antioxidant enzymes (superoxide dismutase (SOD) and AsA peroxidase (APX), etc.) under salt stress was found (Sarker & Oba, 2018a, 2018b, 2020c, 2020e). At the same time the leaves nutritional qualities in the content of protein, ash, energy, dietary fiber, minerals, β–carotene, vitamin C and antioxidants are increases. For this reason, *Amaranthus*

tricolor L. is considered a promising vegetables crop for farmers in areas prone to salinization (Sarker & Oba, 2018d; Sarker et al., 2018; Sarker & Oba, 2020c). It leaves in raw form can be ingredients of salads, soups and sauces, enriching them with biologically active substances, giving them an original taste and color (White & Brown, 2010). *Amaranthus tricolor* L. is used as raw material for the production of food coloring (Gins et al., 2002).

There is an increasing interest among breeders in non–traditional crops such as *Amaranthus* L. (Svirskis, 2003; Sarker et al., 2020; Sarker & Oba, 2020b) and *Actinidia kolomikta* (Rupr. & Maxim.) Maxim (Česonienė & Daubaras, 2007) in recent years. Growing of *Amaranthus tricolor* L. cultivars is commercially and economically profitable in the Moscow region of Russia both in field and in a greenhouse (Pivovarov et al., 2019). The Federal Scientific Center of Vegetable Breeding has selected the *Amaranthus tricolor* cv. 'Valentina'. All vegetative and reproductive organs have a purple–red color of varying intensity. According to the content of amaranthin, they are arranged in the following order: inflorescences (2.2 mg g^{-1}) > leaves (1.4 mg g^{-1}) > stems (0.8 mg g^{-1}) > roots (0.15 mg g^{-1}). As the size increases, the leaf blades change color from red-purple to red-green. (Gins et al., 2002; Kononkov et al., 2018; Platonova et al., 2018).

Many countries grow actinidia species for commercial purposes (Williams et al., 2003). The high nutritional value of actinidia fruits is formed by a complex of biologically active phytochemical (organic and inorganic) components, such as ascorbic acid, phenolic compounds, amino acids, carbohydrates, fiber and minerals (Motyleva et al., 2018). *Actinidia kolomikta* (Rupr. & Maxim.) Maxim is suitable for cultivation in most regions of Russia due to high winter hardiness, early ripening of fruits and a short growing season (Kolbasina et al., 2007). The Federal Scientific Center of Breeding, Agrotechnologies and Nursery has created the *Actinidia kolomikta* cv. 'Narodnaya'.

Both cultivars cv. 'Valentina' (*Amaranthus tricolor* L.) and cv. 'Narodnaya' (*Actinidia kolomikta* (Rupr. & Maxim.) Maxim.) are successfully grown in the Central region of Russia. In previous years, these cultivars were used as models of C3 and C4 plants for comparative evaluation of the leaves physiological and biochemical properties (Motyleva et al., 2021). Knowledge of the leaves anatomical structure, and, in particular, tissue localization of non-photosynthetic pigments and crystals is necessary for further comprehensive and objective assessment of their functional properties. Therefore, we investigated leaves of *Amaranthus tricolor* cv. 'Valentina' and *Actinidia kolomikta* cv. 'Narodnaya' the plants of which which differ significantly in life–forms, anatomical structure and physiological properties.

MATERIALS AND METHODS

A vegetation experiment with amaranth and actinidia plants was conducted during 2020–2021. The plants of both species were grown in natural conditions with artificial protection from precipitation. The experimental site was located at an altitude of 168 m above sea level. Geographical coordinates 55° 7′ 27″ north latitude, 37° 56′ 55″ east longitude. The climate is temperate continental.

Seeds of *Amaranthus tricolor* L. cv. 'Valentina' were sown in boxes. The seedlings were transplanted one by one into plastic pots (with a diameter and height of 250 and 175 mm, respectively). Two-year-old plants *Actinidia kolomikta* (Rupr. & Maxim.) Maxim. cv. 'Narodnaya' were also individually planted into plastic pots (300 and 230 mm in diameter and height, respectively). In total, 20 pots with amaranth and actinidia plants were planted (Fig. 1).
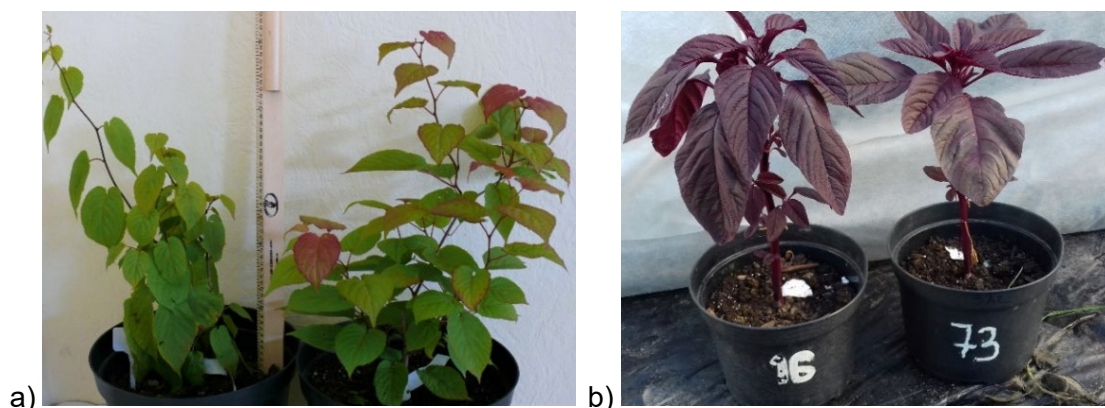

Figure 1. General view of the plants of *Actinidia kolomikta* (Rupr. & Maxim.) Maxim. cv. 'Narodnaya' (a) and *Amaranthus tricolor* L. cv. 'Valentina' (b).

The pots were filled with a mixture of peat and sand (5:1) and had a drainage layer at the bottom. In the pots with the control samples, the substrate moisture was kept at the level of 45–50% for amaranth and 54–60% for actinidia. The soil moisture was determined using the SOIL moisture meter MC–7828 SOIL. Average environmental indicators of the experimental period: day/night temperatures 17.2 °C / 11.7 °C, relative moisture 64%, daytime length 17 h.

The leaves of the middle part were used for all analyzes.

Light microscopy. There were 20 plants taken for every cytological examination. Anatomical analyses were carried out on native material at different stages of ontogenesis without stains and fixatives. Longitudinal and cross sections of fresh matter were cut by hand and microtom (Microm HM 430). Sections were placed in a drop of water, looked and photographed through a 10x or 40x objective of a Zeiss (Jena, Germany) Axiostar plus light microscope equipped with a Digital Camera Canon Power Shot A640 (zoom from 4.0 to 16.0).

Scanning Electron Microscopy. To visualize the microstructure of the adaxial and abaxial surfaces of the leaves, as well as to fulfill the mineral composition of the inclusions, an analytical scanning electron microscope (REM) JEOL JSM–6010 LA (JEOL Ltd, Japan) was used. The die-cuts of 5 mm × 5 mm were taken to the left and right of the central veins from at least 10 leaves and placed on carbon tape mounted on the microscope stage. The cross-sections of the leaves with a thickness of 0.5–1 mm were fixed perpendicular to the surface of the table. The leaves were not pre-treated, as microscopy was carried out under low vacuum conditions (60 Pa) and the deformation of the cross–sections was negligible.

Energy dispersive analysis. The mineral composition was determined by energy dispersion spectrometry (EDS) along with a scanning electron microscope in accordance with the technique of Motyleva (2018) and Motyleva et al. (2021). EDS was used for qualitative and quantitative analysis of available elements in X-ray spectra obtained by scanning the observed image with an electron beam. X-ray microanalysis data were obtained in accordance with standard protocols and included an image of the microstructure of the sample under study, a table of data in weight and atomic percentages, spectra and histograms. An example of spectral data is shown on Fig. 2. Ten measurements were taken for each sample. The local analytical area was 3 mm and the scanning area was at least 12 μm. The mean quadratic deviation did not exceed 1.2–6.9%.
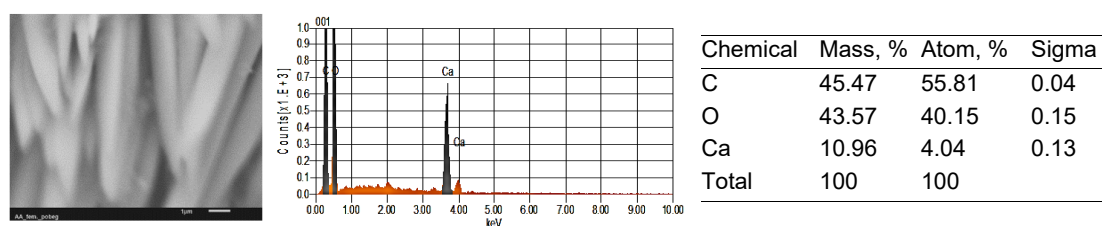

Chemical	Mass, %	Atom, %	Sigma
C	45.47	55.81	0.04
O	43.57	40.15	0.15
Ca	10.96	4.04	0.13
Total	100	100	

Figure 2. The scanned area, the spectrogram and the table of results in the EDS analysis interface.

RESULTS AND DISCUSSION

Actinidia kolomikta (Rupr. & Maxim.) Maxim. cv. 'Narodnaya'

The epidermis cells on both sides of the leaf lamina of *Actinidia kolomikta* (Rupr. & Maxim.) Maxim. cv. 'Narodnaya' have the same irregular, elongated, rarely oval shape (Fig. 3).
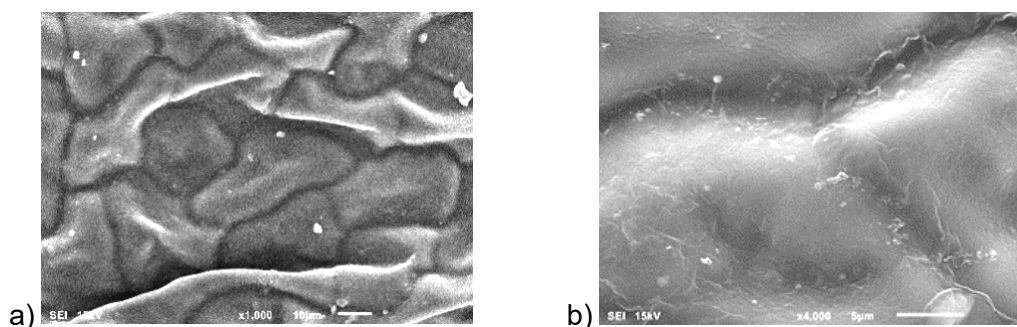

Figure 3. Microstructures of the adaxial surface of *Actinidia kolomikta* (Rupr. & Maxim.) Maxim. cv. 'Narodnaya' leaves under 1,000× (a) and 4,000× (b) magnification.

The abaxial surface is more folded than adaxial. Anomocytic stomata are present only on the abaxial surface. They are located evenly at the level of the leaf surface or slightly buried. There are stomatal characteristics: the length from 12.07 to 16.96 μm, elongated shape, pronounced rings. The wax layer evenly covers the epidermis on both sides of the leaf lamina (Fig. 4). It has smooth or slightly bumpy structure, what is clearly visible at 4,000 x magnification (Figs 3–4).
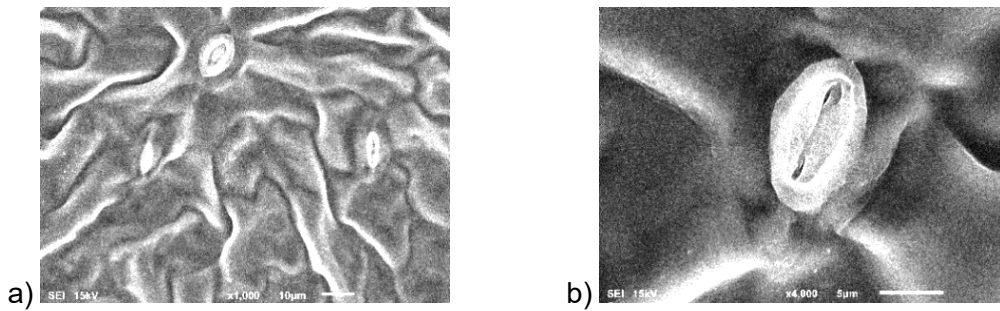
Figure 4. Microstructures of the abaxial surface of *Actinidia kolomikta* (Rupr. & Maxim.) Maxim. cv. 'Narodnaya' leaves under 1,000× (a) and 4,000× (b) magnification.

There are long, multicellular, uniseriate trichomes with an average length of 243.4–375.8 µm on the midrib vein on both sides of the leaf lamina. In addition, rare uniseriate hairs consisting of 2–3 segments are located along secondary veins on the abaxial surface (Fig. 5).
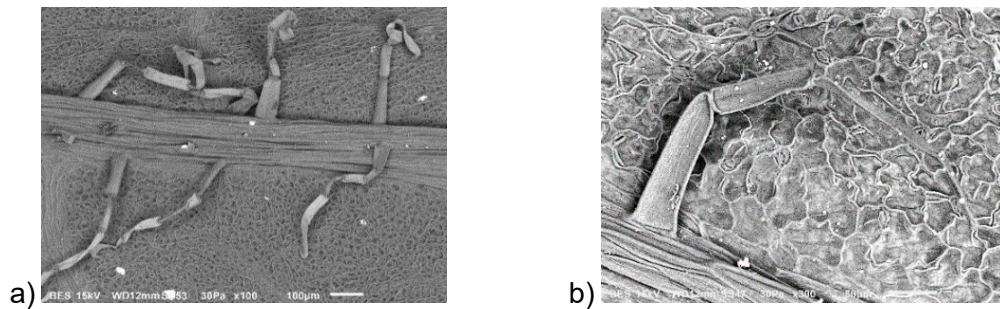

Figure 5. Trichomes of the abaxial surfaces of *Actinidia kolomikta* (Rupr. & Maxim.) Maxim. cv. 'Narodnaya' leaves under 100× (a) and 300× (b) magnification.

Multicellular bristle - like protrusions above a thin vascular bundle are also rarely found there. There are raphids inside these protrusions (Fig. 6).
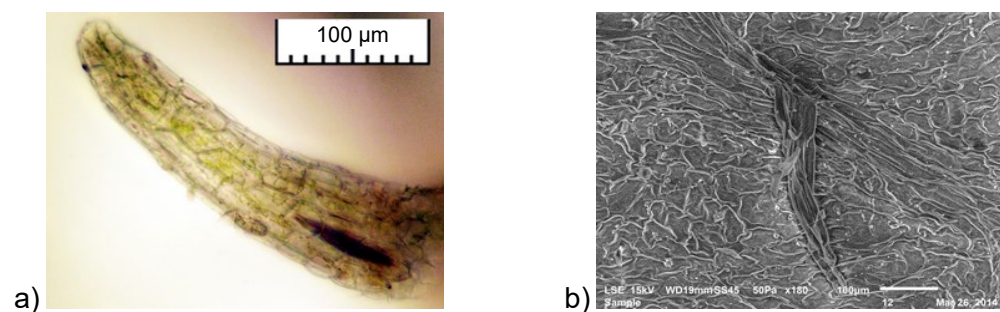

Figure 6. Multicellular bristle - like protrusions of the adaxial surface of *Actinidia kolomikta* (Rupr. & Maxim.) Maxim. cv. 'Narodnaya' leaves.

The leaf blade on the cross sections has a dorsoventral structure. However, the cells of the palisade tissue are tortuous and do not have a clear prismatic shape (Fig. 7, a).

The cross sections show that raphides are deposited in the mesophyll under the epidermis of both sides of the leaf lamina (Fig. 7, b). The plan shows that the raphides are laid mainly along the veins (Fig. 7, c).

Figure 7. Leaf lamina cross sections (a, b) and a plan of the raphids deposition on the abaxial side (c) of leaves of *Actinidia kolomikta* (Rupr. & Maxim.) Maxim. cv. 'Narodnaya'.

Reddish areas may appear on the green leaf under unfavourable conditions. The synthesis of anthocyanins is noted in the epidermis and is often accompanied by trichomes red pigmentation (Fig. 8, a). Anthocyanin cells are also found in the palisade layer (Fig. 8, b).
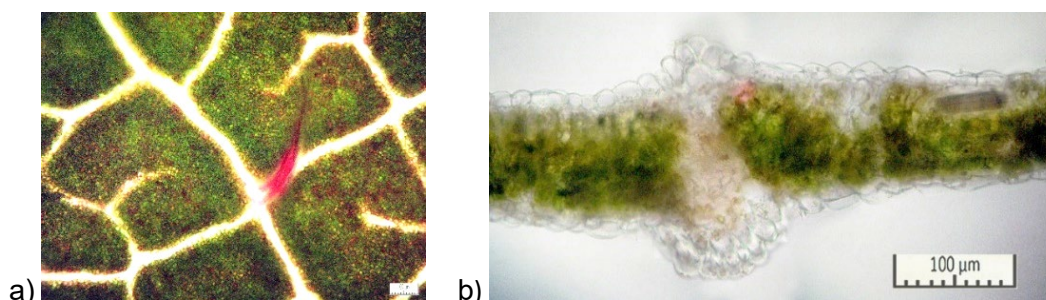

Figure 8. Plan of the adaxial surface (a) and cross section (b) of *Actinidia kolomikta* (Rupr. & Maxim.) Maxim. cv. 'Narodnaya' leaves containing anthocyanins.

The leaf petiole is oval and grooved in cross section (Fig. 9, a). The vascular system of petiole consists of three parts: two upper concentric bundles with an inner xylem and the crescentic vascular strand. In the middle vein of the leaf, separate bundles break off from the crescent (Fig. 9, b).
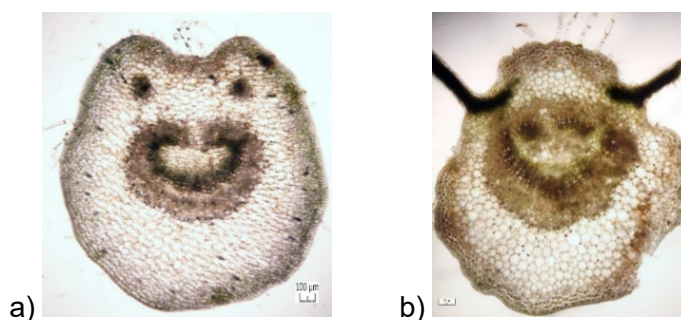

Figure 9. Cross section of the petiole (a) and the midvein (b) of *Actinidia kolomikta* (Rupr. & Maxim.) Maxim. cv. 'Narodnaya' leaves.

The phloem of vascular strand contains raphides. From the outside, the phloem is covered by the single-row starch sheat (endodermis). The cortical parenchyma is collenchymatous.

Raphides are packed together lengthwise in ideoblast cells of cortical parenchyma. Two types of crystals have been found. The first type is represented by needle-shaped crystals with a length of 20–25 µm and a width of 0.4–0.6 µm. The second type is in the form of a rectangular prism with a width of 5.6–6.5 µm (Fig. 10).
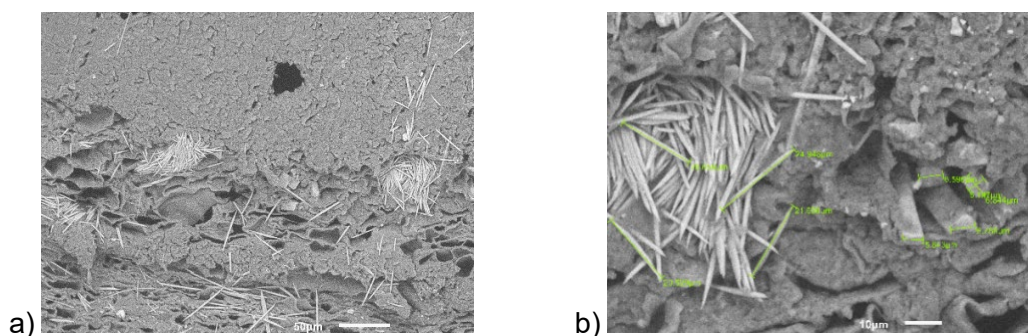

Figure 10. Mineral inclusions on the cross section of the petiole of *Actinidia kolomikta* (Rupr. & Maxim.) Maxim. cv. 'Narodnaya' leaves: needle-shaped crystals (a) and idioblasts (raphides) with needle-shaped crystals (on the left) and rectangular crystals (on the right) (b).

In general, the presented data on the leaf morphological anatomical structure of cv. 'Narodnaya' consistent with the diagnostic characteristics of the *Actinidia kolomikta* (Rupr. & Maxim.) Maxim. (Ferguson, 2011, Motyleva et al., 2017). Of all the wide diversity of trichomes described for *Actinidiaceae* Gilg & Werderm (Watson & Dallwitz, 1992) we observed two types: multicellular, uniseriate hairs and multicellular bristle-like protrusions, containing raphids. The presented description of tissue composition of the petiole cv. 'Narodnaya' generally coincided with that of *Actinidia kolomikta* stem (Roy et al., 2020). Therefore, the presence of a starch sheat in the petioles of cv. 'Narodnaya' is quite logically, since, according to Ferguson (2011), the presence of identical layer in the stem of *Actinidia kolomikta* is a species trait. We believe that the presence of a starch sheat contributes to the high frost resistance of shoots of the *Actinidia kolomikta* compared to other *Actinidia* Lindl. species (Kolbasina et al., 2007). We have noted the appearance of anthocyanin staining of adaxial epidermis cells, trichomes and palisade mesophyll cells in connection with adaptive responses of plants to stress. This pigmentation is not associated with variegated foliage, which is noted during the flowering period (Wang et al., 2015) and may have other chemical profile (Kovinich et al., 2014, 2015).

Amaranthus tricolor L. cv. 'Valentina'

The adaxial surface of leaves of *Amaranthus tricolor* L. cv. 'Valentina' has chaotically arranged segmented trichomes 80–100 µm long and small stomata (8.51 µm). The shape of epidermal cells is irregularly polygonal (Fig. 11).
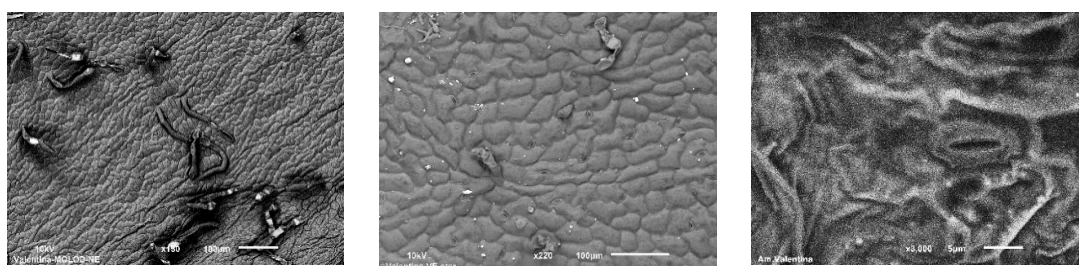
Figure 11. Microstructures of the adaxial surface of *Amaranthus tricolor* L. cv. 'Valentina' leaves under 150×, 220× and 3,500× magnification.

The abaxial surface of leaves of cv. 'Valentina' has small stomata (12.31 µm). Shape of epidermal cells is irregularly polygonal, too (Fig. 12, a, b). Some epidermal cells contain betacyanins predominantly adjacent to the stomata. Cells of abaxial epidermis are most intensively stained than adaxial one (Fig. 12, c).
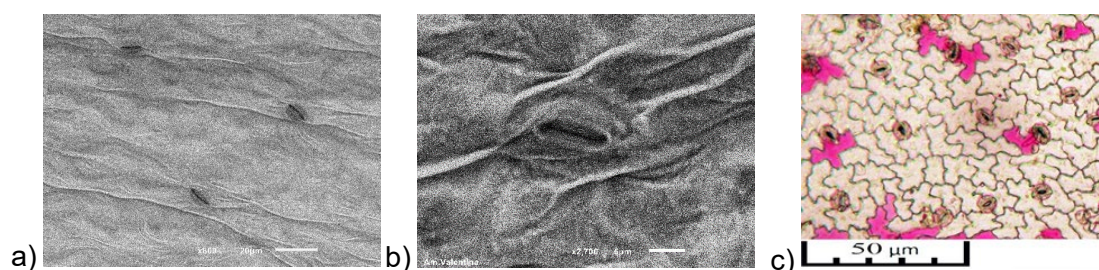

Figure 12. Microstructures of the adaxial surface of *Amaranthus tricolor* L. cv. 'Valentina' leaves under SEM, 100× (a) and 2,700× (b) magnification, and by light microscopy (c).

Leaf lamina on the cross-sections demonstrate the Kranz-type leaf anatomy inherent in C4 plants. All vascular bundles surrounded by a layer of bundles heath cells with centripetally arranged chloroplasts. In addition, there are single-row layers of mesophyll cells under the adaxial and abaxial epidermis. The leaf lamina is characterized by dorsoventral structure, since the adaxial mesophyll cells have a palisade structure and the abaxial one are spongy. Part of the mesophyll cells on both sides of the leaf lamina contain betacyanins. Their presence in the cells vacuoles does not exclude the existence of chloroplasts in the cytoplasm. There are no betacyanins in the bundles heath cells. (Fig. 13).

Figure 13. Cross sections of *Amaranthus tricolor* L. cv. 'Valentina' leaves under light microscopy (a). Kranz-structure: vascular bundles surrounded by a layer of bundle sheath cells. SEM, 900× magnification (b).

Large druses up to 40 microns in diameter are located between the vascular bundles (Fig. 14, a, c). The druse is an aggregate mass of small crystals (Fig.14, c). The SEM image of a cross section of the leaf shows regularly arranged druses. The average distance between the druses is 243.3 μm.
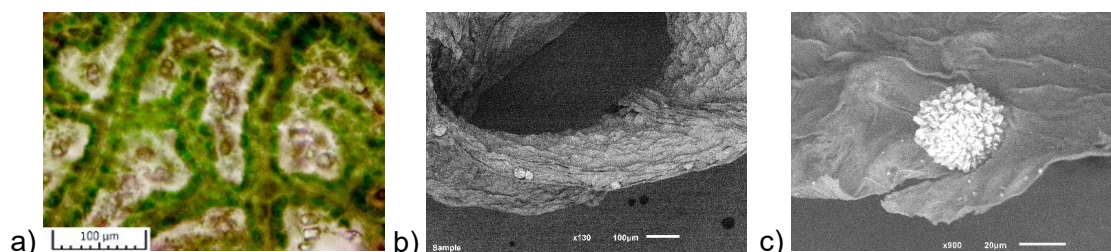

Figure 14. *Amaranthus tricolor* L. cv. 'Valentina' leaves: the plan of druses deposition under light microscopy (a), the cross sections and the druse under SEM, 130× and 900× magnification (b, c).

The petiole is fluted and winged from the middle. On the cross-section the circumference of the petiole on the adaxial side breaks by a deep groove covered with trichomes (Fig. 15, a). Under the epidermis of the petiole is a two- or three-row collenchyma. The collenchyma covers the cortical parenchyma and is interrupted in the area of small furrows where stomata are located. The vascular bundles are scattered in a semicircle around the pith. Outside, they are surrounded by a single-row endodermis brightly pigmented with betacyanins. In addition to the endodermis, cells with betacyanins are found in cortical parenchyma and in the epidermis. They are scattered randomly and condense in areas under the furrows in the cortical parenchyma. Occasionally, the presence of pink pigments in the cells of collenchyma and phloem was noted. The number of vascular bundles at the base of petioles is odd-numbered and variable. We observed from 5 to 13. The petiole passes into the midrib, gradually decreasing in diameter. At the same time, the number of vascular bundles decreases sequentially from the petiole base to the distal tip of the midvein. Collenchyma and endodermis are also gradually disappearing (Fig. 15, b).
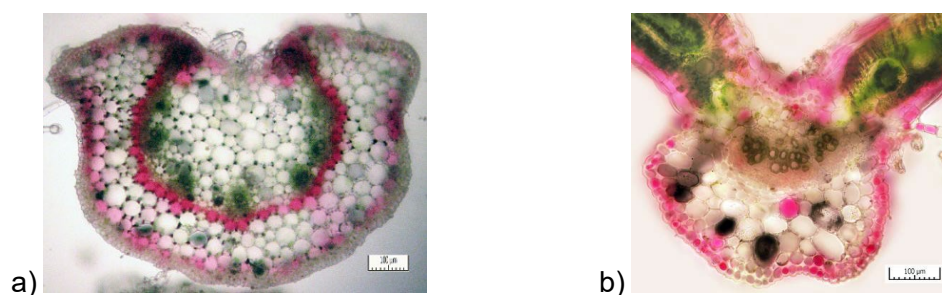

Figure 15. Cross sections of petiole (a) and midvein (b) of *Amaranthus tricolor* L. cv. 'Valentina' leaves (light microscopy).

Trichomes are multicellular, uniseriate, ending in a large oval cell in the distal tip and becoming multiseriate at the base. The hairs often contain betacyanins (Fig. 16).

According to the results of a morphological and anatomical study, we were found that the leaves of *Amaranthus tricolor* L. cv. 'Valentina' have a typical for C2 kranz-type of leaf anatomy. We have clarified the leaves anatomical characteristics of *Amaranthus tricolor* L. made on other samples by Arya et al. (2017), El–Ghamery et al. (2017), Hussain et al. (2018). Our data on the dorsoventral structure of the leaf lamina are coincides with description of Tsutsumi et al. (2017). We have established the variability of the number of vascular bundles at the base of petioles. Similar data were obtained on successive sections of other amaranth species (Timonin, 1984, 2011).
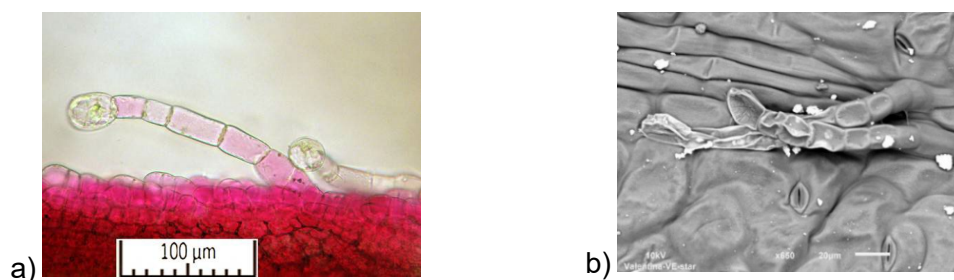

Figure 16. Trihomes of *Amaranthus tricolor* L. cv. 'Valentina' leaves under light microscopy (a) and SEM (b), 650× magnification.

The cortical and pith parenchyma contain idioblasts with crystal sand (Fig. 17).
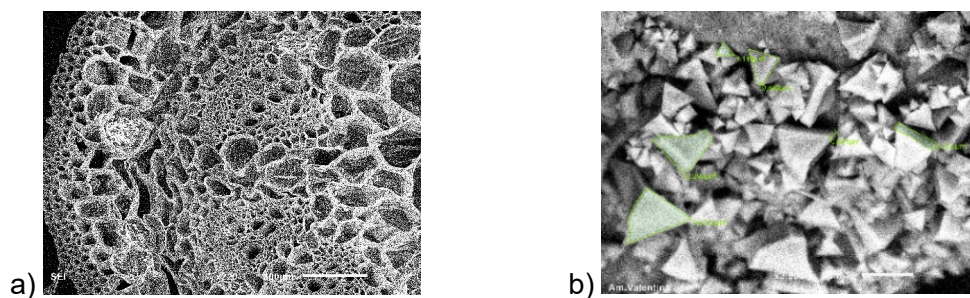

Figure 17. The crystal sand in idioblast among parenchyma cortical cells of the petiole on the cross–section of *Amaranthus tricolor* L. cv. 'Valentina' leaves.

For the first time betacyanins localization in leves of *Amaranthus tricolor* L. has been described. In the leaf lamina they are concentrated in the epidermis and in the mesophyll subepidermal cells. And in the leaf petiole, they are present mainly in endodermis, cortical parenchyma and epidermis. Such betacyanins localization significantly and positively affects the adaptive properties of plants according to the data presented in the introduction.

Visual appearance of plants and anatomical sections of leaves demonstrate that cv. 'Valentina' does not contain betaxanthins. We came to this conclusion due to the fact that we did not observe cells with yellow or orange vacuoles. The results of chemical analysis confirm the data of microscopic studies (Gins et al., 2002; Kononkov et al., 2018; Platonova et al., 2018).

The chemical composition of crystals was studied by the EDS method. According to the results of the analysis, it was found that Ca is the main element of all mineral

351

inclusions in the leaves of both actinidia and amaranth. The highest concentration of Ca in druses and crystal sand have the leaves of amaranth (38.59 and 26.33 mass %, respectively). Druses from the leaf lamina also contain Mg, P and K. Crystall sand from petiole is a typical oxalate, consisting of Ca and K. Actinidia leaf crystals contain Mg, P, Ca, K and Si. Large rectangular crystals contain more Si (3.5 times), Mg (2 times), Ca and K (1.4 times) compared to needle-shaped crystals. But needle-shaped crystals contain P 1.8 times more than rectangular ones. (Table 1).

Table 1. Chemical composition of mineral inclusions of actinidia and amaranth leaves, mass %

Elements	Type of mineral inclusions in leaves of:			
	Amaranthus tricolor L. cv. 'Valentina'		*Actinidia kolomikta* (Rupr. & Maxim.) Maxim. cv. 'Narodnaya'	
	Druses	Crystal sand	Needle-shaped crystal	Rectangular crystal
C	29.61 ± 1.11	28.24 ± 0.87	39.30 ± 1.31	36.23 ± 1.21
O	30.91 ± 0.98	42.65 ± 1.15	45.92 ± 1.43	44.12 ± 1.34
Mg	0.25 ± 0.01	–	0.02 ± 0.005	0.04 ± 0.01
P	0.48 ± 0.04	–	0.11 ± 0.008	0.06 ± 0.01
Ca	38.59 ± 1.14	26.33 ± 1.02	13.67 ± 0.21	18.74 ± 0.22
K	0.16 ± 0.02	2.72 ± 0.04	0.81 ± 0.04	1.12 ± 0.04
Si	–	–	0.02 ± 0.008	0.07 ± 0.01

Notes: – element not detected.

Current studies have shown that Ca^{2+} is a key element in signaling pathways and is mobilized in stressful situations. And the ability to accumulate this element increases the survival and adaptability of cultivars to adverse environmental factors. (Sanders et al., 2002; Reddy & Reddy, 2004; White, 2004).

CONCLUSIONS

So, we have established the features of the anatomical structure of the leaves of C3 and C4 plants on the example of *Actinidia kolomikta* (Rupr. & Maxim.) Maxim. (cv. 'Narodnaya') and *Amaranthus tricolor* L. (cv. 'Valentina'), respectively. The noted features of the leaf petiole tissues in both varieties generally coincide with anatomical characteristics of the stem and leaf petiole of these species according to other authors, and, therefore, are species-specific.

It has been shown that amaranth leaves contain trichomes of one type, but actinidia has two types. Betalains / anthocyanins can accumulate in the leaves trichomes of both species.

The endodermis in the leaf petioles is clearly expressed due to the presence of amyloplasts (in actinidia and amaranth) and betacyanins (in amaranth). The presence of amyloplasts indicates a high adaptability of cultivars, since these inclusions in the endodermis cells are responsible for storing glucose by polymerization and starch reutilization, and also play the role of statolites - georeceptor structures (Fleurat-Lessard, 1981).

Betalains in the leaves of the cv. 'Valentina' (*Amaranthus tricolor* L.) are represented only by betacyanins. Betaxanthins are absent. Betacyanins in leaf blades are deposited in the epidermal and subepidermal layers, but are not present in the bundle sheath. We assume that the established feature of betacyanins localization is due to the

fact that the cells of the bundle sheath and mesophyll differentially express many genes (Bowman et al., 2013). Betacyanins accumulate in the parenchyma and collenchyma cells of leaf petioles. The abundance of betacyanin cells in cortex under stomata can affect transpiration and gas exchange.

It was found that mineral inclusions in the amaranth petioles are present in the form of crystal sand, and are connected into the mineral aggregates - druses in the leaf lamina. The crystall sand contains oxalates of Ca (mainly) and K. There are Mg and P additionally present in the mineral composition of druses.

It should be noted, that cells with raphides in actinidia leaves are mainly located close to or inside the vascular bundles. Raphides with needle-shaped crystals are deposited in the subepidermal layers of the mesophyll along the vascular bundles in leaf lamina and are located in the phloem of petioles. Raphides with needle-shaped and rectangular crystals having an identical elements composition are also deposited in the cortex of leaf petioles. Raphides contain Ca, K, Mg and P, just like amaranth druses, but differ in the presence of Si.

REFERENCES

Bowman, S.M., Patel, M., Yerramsetty, P., Mure, C.M., Zielinski, A.M., Bruenn J.A. & Berry J.O. 2013 A novel RNA binding protein affects rbcL gene expression and is specific to bundle sheath chloroplasts in C4 plants. *BMC Plant Biol*. **13**(138), 24 p. doi: 10.1186/1471–2229–13–138

Arya, S. Rajesh, K.T. & Santhoshkumar, R. 2017. Comparative studies on morphology and anatomy of selected species of the genus *Amaranthus* L. in Kerala. *Indian Journal of Plant Sciences*, **6**(2), 99–105.

Cai, Y.–Z., Sun, M., Wu, H.X., Huang, R.H. & Corke, H. 1998. Characterization and quantification of betacyanin pigments from diverse *Amaranthus* species. *Journal of Agricultural and Food Chemistry* **46**, 2063–2070. doi: 10.1021/JF9709966

Cai, Y.–Z., Sun, M. & Corke, H. 2005 HPLC Characterization of Betalains from Plants in the Amaranthaceae. *Journal of chromatographic science* **43**(9), 454–460 doi: 10.1093/CHROMSCI/43.9.454

Česonienė, L. & Daubaras, R. 2007. Determining of genetic diversity and genetic relationships among Lithuanian selections of *Actinidia kolomikta. Agronomy Research* **5**(1), 13–20.

Chirkova, T.V.1999. Amaranth – the culture of the XXI century. *Soros educational journal* **10**, 22–27 (in Russian).

Clearwater, M.J. & Clark, C.J. 2003. In vivo magnetic resonance imaging of xylem vessel contents in woody lianas. *Plant, Cell and Environment* **26**, 1205–1214. doi: 10.1046/J.1365–3040.2003.01042.X

Close, D.C. & Beadle C.L. 2003. The ecophysiology of foliar anthocyanin. *The Botanical Review* **69**(2), 149–161. doi: 10.1663/0006–8101(2003)069[0149:TEOFA]2.0.CO;2

Condon, J.M. 1992. Aspects of kiwifruit stem structure in relation to transport ISHS. *Acta Horticulturae* **297**, II International Symposium on Kiwifruit: 419–426. doi: 10.17660/ACTAHORTIC.1992.297.55

Crivellaro, A. & Schweingruber F.H. 2015. *Stem Anatomical Features of Dicotyledons. Xylem, phloem, cortex and periderm characteristics for ecological and taxonomical analysis.* Publisher: Kessel Publishing House. 159 pp. ISBN: 978–3–945941–08–9 Corpus ID: 90687506

Durnova, N., Simakova M, Isaev D., I. Simakova I. & Simakov A. 2021. Morphology of *Camellia sinensis* L. leaves as marker of white tea authenticity. *Agronomy Research* **19**(3), 1436–1445. doi: 10.15159/ar.21.126

El–Ghamery, A.A., Sadek, A.M. & Abdelbar, O.H. 2017. Comparative anatomical studies on some species of the genus Amaranthus (Family: Amaranthaceae) for the development of an identification guide. *Annals of Agricultural Sciences* **62**(1), 9 p. doi: 10.1016/j.aoas.2016.11.001

Ferguson, A.R. 2011. Kiwifruit: A Botanical Review. In book: *Horticultural Reviews*, Volume **6**, 1–64. doi: 10.1002/9781118060797.ch1

Flexas, J., Loreto, F. & Medrano, H. 2012. *Terrestrial Photosynthesis in a Changing Environment: A Molecular, Physiological, and Ecological Approach*. Cambridge University Press, 728 pp. doi: 10.1017/CBO9781139051477.002

Franceschi, V.R. & Horner, H.T. 1980. Calcium oxalate crystals in plants. *Bot. Rev.* **46**, 361–427. doi: 10.1007/BF02860532

Fleurat–Lessard, P. 1981. Ultrastructural features of the starch sheath cells of the primary pulvinus after gravistimulation of the sensitive plant (Mimosa pudica L.). *Protoplasma* **105**, 177–184. doi: 10.1007/BF01279216

Gins, M.S., Gins, V.K. & Kononkov, P.F. 2002. Change in the biochemical composition of amaranth leaves during selection for increased amaranthine content. *Applied Biochemistry and Microbiology* **38**(5), 474–479. doi: 10.1023/A:1019980821313

Hoang, L.H., De Guzman, C.C., Cadiz, N.M. & Tran, D.H. 2019. Physiological and phytochemical responses of red amaranth (*Amaranthus tricolor* L.) and green amaranth (*Amaranthus dubius* L.) to different salinity levels. *Legume Research. An International Journal* **470**, 1–6. doi: 10.18805/LR–470

Hussain, A.N., Zafar, M., Ahmad, M., Khan, R., Yaseen, G., Khan, M.S., Nazir, A., Khan, A.M. & Shaheen, S. 2018. Comparative SEM and LM foliar epidermal and palyno-morphological studies of *Amaranthaceae* and its taxonomic implications. *Microsc Res Tech.* **81**(5), 474–485. doi: 10.1002/jemt.23001

Khanam, U.K.S. & Oba, S. 2013. Bioactive substances in leaves of two amaranth species, *Amaranthus tricolor* and *A. hypochondriacus*. *Canadian J. Plant Sci.* **93**, 47–58. doi: 10.4141/CJPS2012–117

Kolbasina, E.I., Solovyova, L.V., Tulnova, N.N., Kozak, N.V., Skripchenko, N.V., Moroz, P.A., Korchemnaya, N.A. & Gvosdezkaya, A.I. 2007. *Cultured Flora of Russia: Actinidia. Schisandra.* Moscow. Rosselhozakademia, pp. 327 (in Russian). ISBN 978-5-85941-258-7

Kononkov, P.F., Gins, M.S. & Gins, V.K. 2018. *Amaranth. Introduction in Russia.* Moscow. Scientific and Publishing Center 'Luch'. 319 pp.

Kovinich, N., Kayanja, G., Chanoca, A., Otegui, M.S. & Grotewold, E. 2015. Abiotic stresses induce different localizations of anthocyanins in *Arabidopsis*. *Plant Signaling & Behavior*, **10**(7), e1027850. doi: 10.1080/15592324.2015.1027850

Kovinich, N., Kayanja, G., Chanoca, A., Riedl, K., Otegui, M.S. & Grotewold, E. 2014. Not all anthocyanins are born equal: distinct patterns induced by stress in *Arabidopsis*. *Planta* **240**, 931–940. doi: 10.1007/s00425–014–2079–1

Lotova, L.I. 2011. *Morphology and anatomy of higher plants*. Editorial URSS, 528 pp. (in Russian). ISBN 5–8360–0140–5

McConn, M.M. & Nakata, P.A. 2002. Calcium oxalate crystal morphology mutants from *Medicago truncatula*. *Planta* **215**, 380–386. doi: 10.1007/s00425–002–0759–8

Motyleva, S.M., Gins, M.S., Kabashnikova, L.F., Kozak, N.V., Tetyannikov, N.V., Mertvischeva, M.E., Domanskaya, I.N. & Pilipovich, T.S. 2021. Drought effects on the physiological and biochemical parameters of *Amaranth* (C–3) and *Actinidia* (C–4) plants. *SABRAO Journal of Breeding and Genetics* **53**(2), 248–262.

Motyleva, S., Kozak, N., Kulikov, I., Medvedev, I. & Imamkulova, Z. 2017. The peculiarities of *Actinidia* species leaves micromorphology. *Agrobiodiversity*, 342–346. doi: 10.15414/agrobiodiversity.2017.2585–8246.342–346

Motyleva, S.M., Kozak, N.V. & Kulikov, I.M. 2018. The low molecular weight metabolites in the water extract of fruits of *Actinidia* Lindl. *Problems Biol. Med. Pharm. Chem.* **10**(21), 91–97. doi: 10.29296/25877313–2018–10–18

Pivovarov, V.F., Gins, M.S. & Gins, V.K. 2019. Economic efficiency of the raw materials production for obtaining a natural food dye from amaranth. *IOP Conference Series Earth and Environmental Science* **395**(1), 012085. doi: 10.1088/1755–1315/395/1/012085

Platonova, S.Y., Peliy, A.F., Gins, E.M. Sobolev, R.V., Vvedenskiy, V.V. 2018. The study of morphological and biochemical parametres of *Amaranthus tricolor* L. Valentina variety. *RUDN Journal of Agronomy and Animal Industries* **13**(1), 7–13. doi: 10.22363/2312–797x–2018–13–1–7–13 (in Russian).

Reddy, V.S. & Reddy, A.S. 2004. Proteomocs of calcium–signalling components in plants. *Phytochem.* **65**, 1745–1776. doi: 10.1016/J.PHYTOCHEM.2004.04.033

Roy, Y.F., Boyko, V.I. & Remen, K.S. 2020. The anatomical structure of the stem of *Actinidia kolomikta* Maxim. in the conditions of south–west Belarus. *Actual problems of the forest complex* **5**, 140–143 (in Russian).

Sanders, D., Pellow, J., Brownlee, C. & Herper, J.F. 2002. Calcium at the crossroads of signaling. *Plant Cell* **1**, 101–417. doi: 10.1105/tpc.002899

Sarker, U. & Oba, S. 2018a. Augmentation of leaf color parameters, pigments, vitamins, phenolic acids, flavonoids and antioxidant activity in selected *Amaranthus tricolor* under salinity stress. *Sci. Rep.* **8**, 12349. doi: 10.1038/s41598–018–30897–6

Sarker, U. & Oba, S. 2018b. Catalase, superoxide dismutase and ascorbate–glutathione cycle enzymes confer drought tolerance of *Amaranthus tricolor*. *Scientific Reports* **8**, 16496. doi: 10.1038/s41598–018–34944–0

Sarker, U. & Oba, S. 2018c. Drought stress effects on growth, ROS markers, compatible Solutes, phenolics, flavonoids, and antioxidant activity in *Amaranthus tricolor*. *Appl. Biochem. Biotechnol.* **186**, 999–1016. doi: 10.1007/ s12010–018–2784–5

Sarker, U. & Oba, S. 2018d. Drought stress enhances nutritional and bioactive compounds, phenolic acids and antioxidant capacity of *Amaranthus* leafy vegetable. *BMC Plant Biol.* **18**, 258. doi: 10.1186/s12870–018–1484–1

Sarker, U. & Oba, S. 2019a. Antioxidant constituents of three selected red and green color *Amaranthus* leafy vegetable. *Scientific Reports.* **9**, 18233. doi: 10.1038/s41598-019-52033-8

Sarker, U. & Oba, S. 2019b. Salinity stress enhances color parameters, bioactive leaf pigments, vitamins, polyphenols, flavonoids and antioxidant activity in selected *Amaranthus* leafy vegetables. *J. Sci. Food Agric.* **99**, 2275–2284. doi: 10.1002/jsfa.9423

Sarker, U. & Oba, S. 2020a. Leaf pigmentation, its profiles and radical scavenging activity in selected *Amaranthus tricolor* leafy vegetables. *Sci. Rep.* **10**, 18617. doi: 10.1038/s41598-020-66376-0

Sarker, U. & Oba, S. 2020b. Nutraceuticals, phytochemicals, and radical quenching ability of selected drought-tolerant advance lines of vegetable amaranth. *BMC Plant Biol.* **20**, 564. doi: 10.1186/s12870-020-02780-y

Sarker, U. & Oba, S. 2020c. Phenolic profiles and antioxidant activities in selected drought-tolerant leafy vegetable amaranth. *Sci. Rep.* **10**, 18287. doi: 10.1038/s41598-020-71727-y

Sarker, U. & Oba, S. 2020d. Polyphenol and flavonoid profiles and radical scavenging activity in leafy vegetable *Amaranthus gangeticus*. *BMC Plant Biol.* **20**, 499. doi: 10.1186/s12870-020-02700-0

Sarker, U. & Oba, S. 2020e. The response of salinity stress–induced *A. tricolor* to growth, anatomy, physiology, non–enzymatic and enzymatic antioxidants. *Front. Plant Sci.* **11**, 559876. doi: 10.3389/fpls.2020.559876

Sarker, U., Hossain, M.N., Iqbal, M.A. & Oba, S. 2020. Bioactive Components and Radical Scavenging Activity in Selected Advance Lines of Salt–Tolerant Vegetable Amaranth. *Front. Nutr.* **7**, 587257. doi: 10.3389/fnut.2020.587257

Sarker, U., Islam, M.T. & Oba, S. 2018. Salinity stress accelerates nutrients, dietary fiber, minerals, phytochemicals and antioxidant activity in *Amaranthus tricolor* leaves. *PLoS ONE* **13**(11), e0206388. doi: 10.1371/journal.pone.0206388

Semenova, G.A. & Romanova, A.K. 2011. Crystals in sugar beet (*Beta vulgaris* L.) leaves. *Cell and Tissue Biology* **53**(1), 74–80 (in Russian). doi: 10.1134/S1990519X11010147

Shu, Z., Shao, L., Huang, H.–Y., Zeng X.–Q., Lin Z.–F., Chen G.–Y. & Peng C.–L. 2009. Comparison of thermostability of PSII between the chromatic and green leaf cultivars of *Amaranthus tricolor* L. *Photosynthetica* **47**, 548–558. doi: 10.1007/s11099–009–0080–x

Solovchenko, A.E. & Merzliak, M.N. 2008. Screening of visible and UV radiation as a photoprotective mechanism in plants. *Russian Journal of Plant Physiology* **55**, 719–737. doi: 10.1134/S1021443708060010

Svirskis, A. 2003. Investigation of amaranth cultivation and utilisation in Lithuania. *Agronomy Research* **1**(2), 253–26.

Timonin, A.K. 1984. Anatomy of the vegetative leaves in some species of the genus Amaranthus L. 2. The leaf blade, petiole and vascular system of the foliar axis. *Byulleten' Moskovskogo Obshchestva Ispytatelei Prirody. Otdel Biologicheskii* **89**(6), 119–127 (in Russian).

Timonin, A.K. 2011. *Anomalous secondary thickening of centrosperms: specificity of morphofunctional evolution of plants*. Association of Scientific Publications KMK. 355 pp. (in Russian).

Tooulakou, G., Giannopoulos, A., Nikolopoulos, D., Bresta, P., Dotsika, E., Orkoula, M.G., Kontoyannis, C.G., Fasseas, C., Liakopoulos, G., Klapa, M.I. & Karabourniotis, G. 2016. Alarm Photosynthesis: Calcium Oxalate Crystals as an Internal CO2 Source in Plants *Plant Physiology* **171**, 2577–2585. doi: 10.1104/pp.16.00111

Tsutsumi, N., Tohya, M., Nakashima, T. & Ueno O. 2017. Variations in structural, biochemical, and physiological traits of photosynthesis and resource use efficiency in Amaranthus species (NAD–ME–type C4). *Plant Production Science* **20**(3), 300–312. doi: 10.1080/1343943X.2017.1320948

Wang, Z.–X., Fan, S.–T., Chen, L., Zhao, Y., Yang, Y.–M., Ai, J., Li, X.–Y., Liu, Y.–X. & Qin, H.–Y. 2015. *Actinidia kolomikta* leaf colour and optical characteristics. *Biologia plantarum* **59**(4), 767–772. doi: 10.1007/s10535–015–0544–8

Watson, L. & Dallwitz, M.J., 1992 onwards. *The families of flowering plants: descriptions, illustrations, identification, and information retrieval*. Version: 20th October 2021. delta–intkey.com.

White, P.J. 2004. Calcium signals in root cells: the roles of plasma membrane calcium channels. *Biologia* **59**(S3), 77–83.

White, P.J. & Brown, P.H. 2010. Plant nutrition for sustainable development and global health. *Ann. Bot.* **105**(7), 1073–1080. doi: 10.1093/aob/mcq085

Williams, M.H., Boyd, L.M., McNeilage, M.A., MacRae, E.A., Ferguson, A.R., Beatson, R.A. & Martin, P.J. 2003. Development and commercialization of 'Baby Kiwi' (*Actinidia arguta* Planch.). *Acta Hort.* **610**, 81–86. doi: 10.17660/ACTAHORTIC.2003.610.8

Zhigila, D., Yuguda, U., Akawu, J. & Oladele, F. 2014. Palynomorphs and floral bloom as taxonomic characters in some species of the genus *Amaranthus* L. (*Amaranthaceae*). *Bayero Journal of Pure and Applied Sciences* **7**, 164–168. doi: 10.4314/BAJOPAS.V7I2.29